

# Predicting the Mo substitution and vacancy-complex induced electrical defect levels in Ge

E. Igumbor<sup>1,2</sup>, O. Olaniyan<sup>1</sup>, R. E Mapasha<sup>1</sup>, H. T. Danga<sup>1</sup>, W. E. Meyer<sup>1</sup>

<sup>1</sup> Department of Physics, University of Pretoria, Pretoria 0002, South Africa

<sup>2</sup> Department of Mathematical and Physical Sciences, Samuel Adegoyega University, Km 1 Ogwa-Ehor Rd. Ogwa Edo State Nigeria

E-mail: [wmeyer@up.ac.za](mailto:wmeyer@up.ac.za); [elgumuk@gmail.com](mailto:elgumuk@gmail.com)

**Abstract.** In this report, results based an *ab initio* calculation of Mo substitution and vacancy–complex induced electrical levels in the Ge were presented. Density functional theory with the Heyd, Scuseria and Ernzerhof (HSE06) hybrid functional was used to calculate the total energies of Mo vacancy-complexes of Ge ( $V_{Ge}Mo_{Ge}$ ) and Mo substitution in Ge ( $Mo_{Ge}$ ). Formation and minimum energies of the first nearest neighbour (N1), second nearest neighbour (N2) and third nearest neighbour (N3) configurations of the  $V_{Ge}Mo_{Ge}$  and the  $Mo_{Ge}$  were obtained for charge states  $-2$ ,  $-1$ ,  $0$ ,  $+1$  and  $+2$ . The calculated formation energies for the  $V_{Ge}Mo_{Ge}$  resulted in positive binding energies for the N1, N2 and N3 configurations. For the neutral charge state, the N2 configuration is the most energetically favourable with energy of formation and binding energy of  $-0.14$  and  $0.06$  eV, respectively. The  $Mo_{Ge}$  in the neutral charge state had a formation energy of  $-2.99$  eV and induced electrically active level which exhibits a negative-U ordering within the band gap of Ge. The  $(+2/-1)$  transition state induced by the  $Mo_{Ge}$  is a deep level lying at  $E_V + 0.31$  eV.

## 1. Introduction

Experimental or theoretical studies of defects in germanium (Ge) have been on the increase recently due to the potential application of Ge in microelectronics [1]. The investigation of Ge as a possible promising material for optoelectronic applications and complementary metal–oxide–semiconductor (CMOS) field–effect transistor devices has been on the increase [1]. Ge is a semiconductor that has a narrow indirect band gap of  $0.78$  eV at  $0$  K [2]. Furthermore, due to Ge relatively high electron-hole mobility, it has the potential to be considered as a superior material than silicon for the development of metal-oxide–semiconductor field–effect–transistors (MOSFETs) [3]. Defects are known to influence Ge either positively or negatively. Defects that influence Ge positively, enhances its performance, for example the p– or the n–type dopant which are responsible for the change of the majority carrier type are always desired. Several defects in Ge have been investigated using experimental techniques such as deep level transient spectroscopy (DLTS) [3, 4, 5] or perturbed angular correlation spectroscopy (PACs) [6]. Theoretically, few of these defects have been predicted owing to the shortfall of the density functional theory (DFT) [7] with either local density approximation (LDA) or generalised gradient approximations (GGA) of Perdew, Burke, and Ernzerhof (PBE) [8] in predicting accurately the band gap of Ge. But since the advent of the Heyd, Scuseria and Ernzerhof

(HSE) [9] hybrid functional, this limitation has been eliminated. Amongst the defects in Ge predicted are self, di-interstitials [10], mono or multi-vacancies and recently, rare earth related defects [11, 12, 13]. Experimental or theoretical results have revealed or predicted, that dopants in Ge are known to form clusters with lattice vacancies [14] as a result of defect–complexes in Ge such as vacancy–complexes, interstitial–complexes. Recently it has been shown that negative-U ordering could arise from a Tm defect-complexes in Ge [15].

In this report, the electrical levels induced by Mo vacancy-complexes ( $V_{Ge}Mo_{Ge}$ ) and Mo substitution ( $Mo_{Ge}$ ) in Ge are presented with a view of providing experimental insight for the engineering of these defects for better industrial or laboratory applications. The density functional theory with the HSE06 hybrid functional was used for all calculations. The formation and minimum energies of the first nearest neighbour (N1), second nearest neighbour (N2) and third nearest neighbour (N3) configurations for the  $V_{Ge}Mo_{Ge}$  and the  $Mo_{Ge}$  were obtained for charge states  $-2$ ,  $-1$ ,  $0$ ,  $+1$  and  $+2$ .

## 2. Computational details

All calculations were carried out using HSE06 within the framework of DFT as implemented in the VASP 5.3 code [16]. The projector-augmented wave method [17, 18] was used to separate the valence from the core electrons. Based on the HSE06 approach, the short-range exchange potential was calculated by mixing a 25 percent fraction of nonlocal Hartree-Fock exchange with the GGA-PBE. The HSE06 functional gives accurate predictions of the electronic band gap and improve charge state transition properties for several defects in a semiconductor material [2, 10]. For the modelling of the defects, an initial 64 atom supercell was used for the pristine, while for the  $Mo_{Ge}$  a Ge atom was replaced by a Mo atom in the initial 64 atoms supercell. For the  $V_{Ge}Mo_{Ge}$ , a vacancy was created from the  $Mo_{Ge}$  system to yield Mo vacancy-complex system. A  $2 \times 2 \times 2$  Monkhorst-Park [19] mesh scheme for generating the k-points was used to sample the Brillouin zones. Geometric relaxation was performed until the Hellmann-Feynman forces on each atom and the final change in the total energy were less than  $0.001 \text{ eV}/\text{\AA}$  and  $10^{-5} \text{ eV}$ , respectively. Spin orbit coupling was taken into account for all calculations. While formation energies of the  $V_{Ge}Mo_{Ge}$  and  $Mo_{Ge}$  were calculated using the method of Refs [1, 11], the binding energies for the N1, N2 and N3 configurations of the  $V_{Ge}Mo_{Ge}$  were calculated based on the method of Refs [15, 20]. The effect of using a supercell and its image repetitions gives rise to spurious interactions. Furthermore, the introduction of a charge state in the defect, causes electrostatic interaction problems between the periodic cell containing the defect giving rise to errors. These errors were properly corrected using the FNV method as stated in Refs [1, 11]. The band gap of  $0.78 \text{ eV}$  for Ge as reported by Igumbor *et al* [10] was used for this present report.

## 3. Results and Discussion

Figs 1 and 2 display the fully relaxed geometric structures of the  $Mo_{Ge}$  and  $V_{Ge}Mo_{Ge}$ , respectively. The effects of the defect on the structural properties of both  $V_{Ge}Mo_{Ge}$  and  $Mo_{Ge}$  were examined. Based on a previous report, the experimental and theoretical results of the nearest neighbour Ge–Ge bond length and Ge–Ge–Ge bond angle after structural relaxation were  $2.46 \text{ \AA}$  and  $109.40^\circ$  [14, 20], respectively. For the  $Mo_{Ge}$ , the Mo formed bond length of  $2.49 \text{ \AA}$  with its nearest neighbour Ge atom. The smallest angle formed by two nearest neighbour Ge atoms with Mo is  $109.5^\circ$ . The bond length of Mo–Ge was 1.20% higher than that of the Ge–Ge, and the bond angle of Ge–Mo–Ge was 0.10% higher than that of the Ge–Ge–Ge. This is expected as the atomic radius of the Mo atom is higher than that of the Ge atom. The bond length formed by Ge–Mo and bond angle formed by Ge–Mo–Ge for N1 (N2) were  $2.50$  ( $2.47$ )  $\text{\AA}$  and  $108.14^\circ$  ( $108.52^\circ$ ), respectively. The bond length of the nearest Ge–Mo and the smallest bond angle of the nearest Ge–Mo–Ge for the N3 configuration are similar to that of the

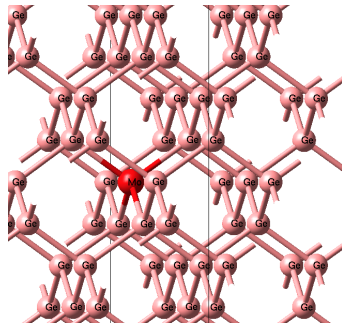


**Figure 1.** Fully relaxed geometric structures of  $\text{MoGe}$ .

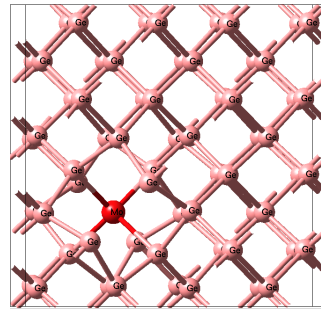


**Figure 2.** Fully relaxed geometric structures of  $\text{V}_{\text{Ge}}\text{MoGe}$  for the N1 configuration.

N1 configuration. Based on the amount of strain induced by the dopant in the system, it is expected that the  $\text{MoGe}$  will induce smaller strain in the system compared to the  $\text{V}_{\text{Ge}}\text{MoGe}$ .

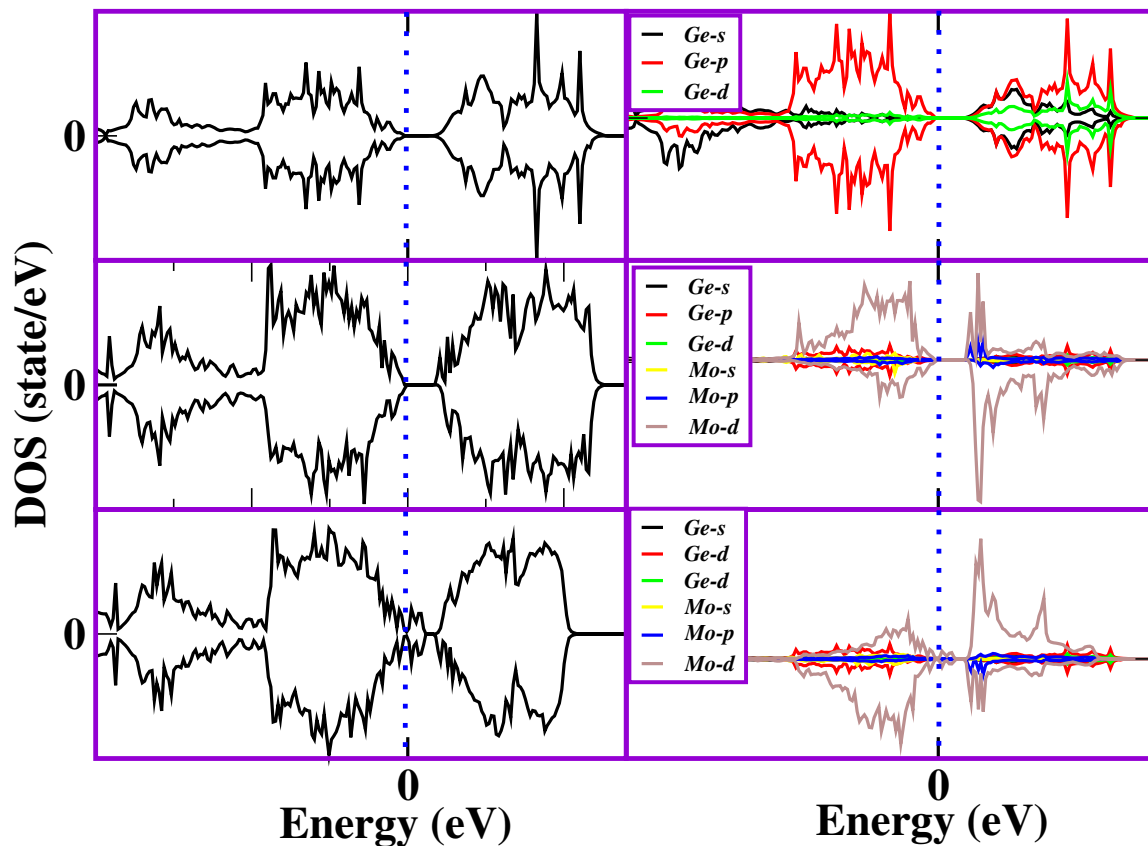


**Figure 3.** The plots of the total density of states (left) and partial density of states (right) for the pristine Ge (upper panel),  $\text{MoGe}$  (middle panel) and  $\text{V}_{\text{Ge}}\text{MoGe}$  (lower panel) complex for the N1 configuration.

Fig. 3 displays the plots of the total density of states (TDOS) and partial density of states (PDOS) of the pristine Ge,  $\text{MoGe}$  and  $\text{V}_{\text{Ge}}\text{MoGe}$  complex (we only displayed the TDOS and

PDOS for the N1 configuration, since the other configurations have similar DOS and PDOS). The TDOS and PDOS for the N2 and N3 configurations are similar to that of the N1 and hence we did not display them. As expected, the  $p$ -orbital is dominant in the band structure for the pristine Ge. The  $\text{Mo}_{\text{Ge}}$  as a result of the  $d$ -orbital from the Mo atom has its ground states orbital densely populated at the valence band maximum. This resulted in the band gap of the pristine Ge reduced by 0.20 eV. The effect of the  $s$  and  $p$ -orbitals of the Mo atom is minimal at the valence band maximum. Another interesting feature observed from the  $\text{Mo}_{\text{Ge}}$  is the presence of strong orbital hybridization between the  $p$ -orbital of Ge and  $d$ -orbital of Mo (see the middle panel of Fig. 3). Both the TDOS and PDOS of the  $\text{V}_{\text{Ge}}\text{Mo}_{\text{Ge}}$  are displayed at the lower panel of Fig. 3. The  $\text{V}_{\text{Ge}}\text{Mo}_{\text{Ge}}$  electrons induced states in the band gap of Ge. These states are about 0.58 eV above the Fermi level. This behaviour is attributed to the influence of the germanium vacancy on the band gap of Ge. The orbital ground states were mainly contributed by the  $d$ -orbital of Mo atom. This led to a reduction in the band gap of Ge by 0.23 eV. The  $\text{V}_{\text{Ge}}\text{Mo}_{\text{Ge}}$  exhibited strong orbital hybridization between the  $p$ -orbital of Ge and the  $d$ -orbital of Mo.

The formation energies of the  $\text{Mo}_{\text{Ge}}$  for  $-2$ ,  $-1$ ,  $0$ ,  $+1$  and  $+2$  were  $-1.97$ ,  $-2.83$ ,  $-2.99$ ,  $-3.45$  and  $-2.81$  eV, respectively. While the formation energies of the  $\text{V}_{\text{Ge}}\text{Mo}_{\text{Ge}}$  for N1, N2 and N3 in the neutral charge state were  $-0.06$ ,  $-0.14$  and  $-0.05$  eV, respectively. Under equilibrium conditions, the N2 amongst other complexes is the most energetically favourable with a formation energy of  $-0.12$  eV. The binding energies (0.06, 0.14 and 0.05 eV of the N1, N2 and N3, respectively) for the  $\text{V}_{\text{Ge}}\text{Mo}_{\text{Ge}}$  have been calculated to predict if the defect-complex is stable without dissociating into non-interacting defects. It turns out that all the calculated binding energies for the N1, N2 and N3 were positive and hence stable. The implication is that the defect complex system of the  $\text{V}_{\text{Ge}}\text{Mo}_{\text{Ge}}$ , remain as cluster defects without dissociating into a non-interacting defect except at the expense of higher energy.

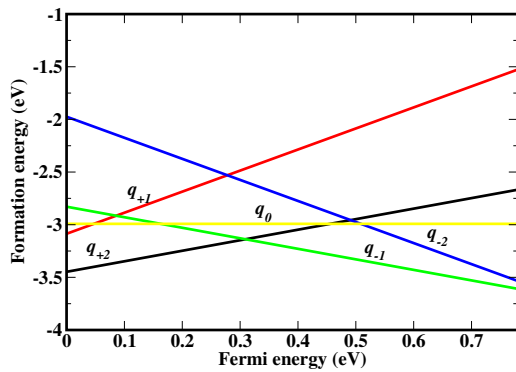


**Figure 4.** Plot of formation energy as a function of the Fermi energy for (a)  $\text{Mo}_{\text{Ge}}$ .

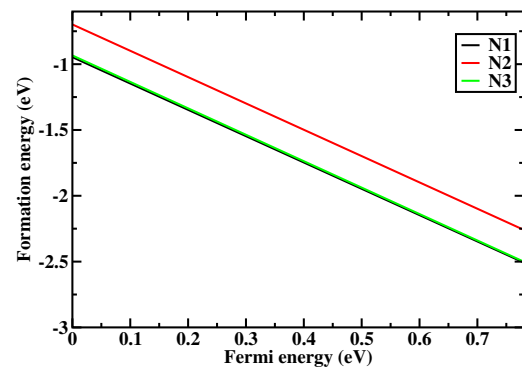


**Figure 5.** Plot of formation energy as a function of the Fermi energy for  $\text{V}_{\text{Ge}}\text{Mo}_{\text{Ge}}$ .

Figs 4 and 5 show the plot of the formation energy as a function of the Fermi energies for the  $\text{Mo}_{\text{Ge}}$  and  $\text{V}_{\text{Ge}}\text{Mo}_{\text{Ge}}$ , respectively. The electrically active levels induced by Mo dopant were investigated for both the  $\text{V}_{\text{Ge}}\text{Mo}_{\text{Ge}}$  and  $\text{Mo}_{\text{Ge}}$ . For any given Fermi energy, it is important to note that a system is assumed to reach thermodynamic equilibrium at the lowest energy charge state. For the  $\text{V}_{\text{Ge}}\text{Mo}_{\text{Ge}}$  no sign of induced electrical level in the band gap of Ge was observed for all configurations. However, the  $-2$  charge state was most thermodynamically stable for all Fermi energies in all configurations. Furthermore, for the  $\text{Mo}_{\text{Ge}}$ , as the Fermi energy is varied, the dopant introduced deep electrically active level in the band gap of Ge. The deep level introduced by the  $\text{Mo}_{\text{Ge}}$  is 0.31 eV above the valence band maximum. Another

interesting feature of  $\text{Mo}_{\text{Ge}}$  is the  $(+2/-1)$  charge state transition level which is a negative-U. Using the method of Ref. [21], we predicted a negative-U ordering with an energy of  $-3.28$  eV. This negative-U is attributed to the large lattice distortion experienced by the defect system. Additional notable thermodynamic charge states transition levels induced in the band gap of Ge due to its doping by Mo are  $(+2/-1)$  and  $(0/-1)$ . However, these levels were thermodynamically accessible but not stable.

#### 4. Summary

The Mo substitution ( $\text{Mo}_{\text{Ge}}$ ) and vacancy-complexes ( $\text{V}_{\text{Ge}}\text{Mo}_{\text{Ge}}$ ) induced electrical levels in Ge were presented. The HSE06 hybrid functional within the framework of DFT was used for all calculations. The formation energy for the neutral charge state of the  $\text{Mo}_{\text{Ge}}$  is  $-2.99$  eV. The  $\text{Mo}_{\text{Ge}}$  induced deep level in the band gap of Ge. The  $\text{Mo}_{\text{Ge}}$  exhibits negative-U ordering for the  $(+2/-1)$  transition. The formation energy result for the  $\text{V}_{\text{Ge}}\text{Mo}_{\text{Ge}}$  show that under equilibrium conditions, the N2 configuration is the most energetically favourable. The  $\text{V}_{\text{Ge}}\text{Mo}_{\text{Ge}}$  did not induce any thermodynamically stable transition charge state level in the band gap of Ge.

#### Acknowledgments

This work is based on the research supported partly by National Research foundation (NRF) of South Africa (Grant specific unique reference number (UID) 98961 ). The opinions, findings and conclusion expressed are those of the authors and the NRF accepts no liability whatsoever in this regard.

#### Reference

- [1] Igumbor E and Meyer W E 2016 *Materials Science in Semiconductor Processing* **43** 129–133
- [2] Deák P, Aradi B, Frauenheim T, Janzén E and Gali A 2010 *Phys. Rev. B* **81** 153203
- [3] Claeys C and Simoen E 2011 *Germanium-based technologies: from materials to devices* (Elsevier)
- [4] Auret F, Coelho S, Myburg G, van Rensburg P J and Meyer W 2009 *Physica B: Condensed Matter* **404** 4376–4378
- [5] Markevich V P, Hawkins I D, Peaker A R, Litvinov V V, Murin L I, Dobaczewski L and Lindström J L 2002 *Applied Physics Letters* **81** 1821–1823
- [6] Igumbor E 2017 *Hybrid functional study of point defects in germanium* Ph.D. thesis University of Pretoria
- [7] Hohenberg P and Kohn W 1964 *Phys. Rev.* **136** B864–B871
- [8] Perdew J P, Burke K and Ernzerhof M 1996 *Phys. Rev. Lett.* **77** 3865–3868
- [9] Heyd J, Scuseria G E and Ernzerhof M 2006 *The Journal of Chemical Physics* **124**
- [10] Igumbor E, Ouma C, Webb G and Meyer W 2016 *Physica B: Condensed Matter* **480** 191–195
- [11] Igumbor E and Andrew R Cand Meyer W E 2017 *Journal of Electronic Materials* **46** 1022–1029
- [12] Igumbor E, Omotoso E, Danga H, Tunhuma S and Meyer W 2017 *Nuclear Instruments and Methods in Physics Research Section B: Beam Interactions with Materials and Atoms* **409** 9 – 13
- [13] Igumbor E, Omotoso E, Tunhuma S, Danga H and Meyer W 2017 *Nuclear Instruments and Methods in Physics Research Section B: Beam Interactions with Materials and Atoms* **409** 31 – 35
- [14] Chroneos A, Uberuaga B P and Grimes R W 2007 *Journal of Applied Physics* **102** 083707
- [15] Igumbor E, Mapasha R E, Andrew R and Meyer W E 2016 *Computational Condensed Matter* **8** 31–35
- [16] Kresse G and Furthmüller J 1996 *Computational Materials Science* **6** 15 – 50
- [17] Kresse G and Furthmüller J 1996 *Phys. Rev. B* **54** 11169–11186
- [18] Blochl P E 1994 *Phys. Rev. B* **50** 17953–17979
- [19] Monkhorst H J and Pack J D 1976 *Phys. Rev. B* **13** 5188–5192
- [20] Igumbor E and Mapasha R E and Meyer W E 2016 *Journal of Electronic Materials* 1–8
- [21] Igumbor E, Obodo K and Meyer W E 2015 *Solid State Phenomena* **242** 440–446